Title
S-nitrosylation of Cofilin-1 Serves as a Novel Pathway for VEGF-Stimulated Endothelial Cell Migration

Journal
Journal of Cellular Physiology, 230(2)

ISSN
0021-9541

Authors
Zhang, Hong-Hai
Wang, Wen
Feng, Lin
et al.

Publication Date
2015-02-01

DOI
10.1002/jcp.24724

Peer reviewed

HHS Public Access

Author manuscript

J Cell Physiol. Author manuscript; available in PMC 2022 March 09.

Published in final edited form as:

J Cell Physiol. 2015 February ; 230(2): 406–417. doi:10.1002/jcp.24724.

S-nitrosylation of Cofilin-1 Serves as a Novel Pathway for VEGF-Stimulated Endothelial Cell Migration

HONG-HAI ZHANG[1], **WEN WANG**[1], **LIN FENG**[1], **YINGYING YANG**[2], **JING ZHENG**[3], **LAN HUANG**[2], **DONG-BAO CHEN**[1,*]

[1] Department of Obstetrics and Gynecology, University of California, Irvine, California

[2] Department of Biophysics and Physiology, University of California, Irvine, California

[3] Department of Obstetrics and Gynecology, University of Wisconsin-Madison, Madison, Wisconsin

Abstract

Nitric oxide (NO) derived from endothelial NO synthase (eNOS) mediates vascular endothelial growth factor (VEGF)-stimulated endothelial cytoskeleton remodeling and migration; however, the underlying mechanisms are elusive. Covalent adduction of a NO moiety ($NO^{\bullet}$) to cysteines called S-nitrosylation (SNO) is a key NO signaling pathway. The small actin-binding protein cofilin-1 (CFL1) is essential for actin cytoskeleton remodeling. We investigated whether S-nitrosylation regulates CFL1 function and endothelial cytoskeleton remodeling and migration upon VEGF stimulation. VEGF rapidly stimulated S-nitrosylation of CFL1, which was blocked by NO Synthase inhibition and eNOS knockdown by specific eNOS-siRNA. Cys80 and Cys139 were identified as the major *SNO*-sites in CFL1 by LC-MS/MS. The actin severing activity of recombinant *SNO*-mimetic CFL1 (C80/139A DMA-CFL1), but not *SNO*-deficient CFL1 (C80/139S DMS-CFL1), was significantly greater than that of wild-type CFL1 (wt-CFL1). When wt-CFL1 and its mutants were overexpressed in endothelial cells, basal actin bound wt-CFL1 was undetectable but significantly increased by VEGF; basal actin bound DMA-CFL1 was readily high and basal actin bound DMS-CFL1 was detectable but low, and both were unresponsive to VEGF. Treatment with VEGF significantly increased filamentous (F-) actin and filopodium formation and cell migration in endothelial cells. Overexpression of wt-CFL1 inhibited VEGF-induced F-actin formation. Overexpression of DMA but not DMS CFL1 decreased basal but not VEGF-stimulated F-actin formation. Overexpression of DMA but not DMS CFL1 suppressed VEGF-stimulated filopodium formation and migration in endothelial cells. Thus, S-nitrosylation of CFL1 provides a novel signaling pathway *post*-NO biosynthesis via eNOS-derived NO for endothelial cytoskeleton remodeling and migration upon VEGF stimulation.

Endothelial cell migration is essential for vasculogenesis and angiogenesis (Lamalice et al., 2007). This motile process is regulated by a myriad of cellular and molecular events, including cytoskeleton remodeling, membrane ruffling, lamellipodium/filopodium formation

*Correspondence to: Dong-bao Chen, Department of Obstetrics and Gynecology, University of California, Irvine, CA 92697. dongbaoc@uci.edu.

The authors have no financial interests to disclose.

(Stupack et al., 2000; Vicente-Manzanares and Horwitz, 2011). It requires the activation of many signaling pathways that converge on cytoskeleton remodeling, followed by a series of events in which the endothelial cells extend, contract, and throw their rear toward the front and progress forward. Cogent evidence has accumulated to demonstrate a critical role of nitric oxide (NO) derived from endothelial NO synthase (eNOS) in mediating endothelial cell proliferation and migration during angiogenesis by stimulation with various angiogenic factors, including vascular endothelial growth factor (VEGF) (Krause et al., 2011; Thachil, 2011; Chen and Zheng, 2014). VEGF stimulates the accumulation of stress fibers in association with new actin polymerization and rapid formation of focal adhesions at the ventral surface of endothelial cells (Liao et al., 2009b). However, the pathways *post*-NO biosynthesis by which VEGF regulates these cellular processes are largely unknown.

Generation of the second messenger cyclic guanosine monophosphate (*cGMP*) is the best defined NO signaling (Arnold et al., 1977); however, many NO bioactivities are cGMP-independent. NO can directly modulate protein function *post*-translationally (Hess et al., 2005). Covalent adduction of a NO moiety ($NO^{\bullet}$) to reactive cysteines is called S-nitrosylation (SNO). Reactive cysteines are often present in the catalytic active sites of a wide range of enzymes (Bartlett et al., 2002). Functional proteomics studies have recently identified hundreds of *SNO*-proteins, consistently supporting a crucial role of S-nitrosylation in regulating the function of proteins that are essential for cardioprotection, G-protein coupled receptor signaling, apoptosis, and angiogenesis, etc. (Hess et al., 2005).

Cofilin-1 (CFL1) is a small actin binding protein essential for actin dynamics during numerous cellular events including cell proliferation and migration (Chrzanowska-Wodnicka et al., 2008). The primary function of CFL1 is to regulate cytoskeleton remodeling via depolymerizing/severing actin filaments (Theriot, 1997). The activity of CFL1 is known to be regulated via phosphorylation/de-phosphorylation on Ser-3, with phosphorylated form being inactive (Kobayashi et al., 2006). When dephosphorylated, CFL1 severs the filamentous (F-) actin to produce free barber ends that are critical for the formation of newborn actin fibers (Condeelis, 2001). We and others have identified CFL1 to be a major *SNO*-target (Dall'Agnol et al., 2006; Han and Chen, 2008; Zhang et al., 2010, 2012). However, whether S-nitrosylation regulates CFL1 function has not been reported.

The objective of this study was to investigate the functional significance of S-nitrosylation of CFL1. We hypothesized that S-nitrosylation of CFL1 plays a crucial role in VEGF-stimulated endothelial cytoskeleton remodeling and migration. Our data show that S-nitrosylation of CFL1 suppresses VEGF-stimulated filopodium formation and cell migration via increasing the actin severing activity of CFL1, thereby providing a novel signaling pathway *post*-NO biosynthesis via eNOS-derived NO for mediating VEGF-stimulated endothelial cell migration.

Materials And Methods

Chemicals and antibodies

Anti-Flag and FITC-labeled anti-Flag antibodies, bovine serum albumin (BSA), 4-(2-hydroxyethyl)-1-piperazineethane-sulfonic acid (HEPES), *N*-nitro-L-arginine-methylester

(L-NAME), *N*-nitro-D-arginine-methylester (D-NAME), and all other chemicals unless specified, were from Sigma (St Louis, MO). *N*-[6-(biotinamido) hexyl]-3'-(2'-pyridyldithio) propionamide (biotin-HPDP) was from Thermo scientific (Rockford, IL). S-nitrosoglutathione (GSNO) was from Cayman (Ann Arbor, MI). Anti-CFL1 antibody was from Abcam (San Francisco, CA). Anti-β-actin monoclonal antibody was from Ambion (Austin, TX). Anti-eNOS antibody was from Santa Cruz Biotechnology, Inc (Santa Cruz, CA). Prolong Gold antifade reagent with 4',6-diamidino-2-phenylindole, MCDB131 and M199 were from Invitrogen (Carlsbad, CA).

Cell isolation, culture, and treatment

Ovine fetoplacental artery and uterine artery endothelial cells (*i.e.*, oFPAEC and UAEC) were isolated from pregnant ewes and validated as described previously (Chen et al., 2004; Liao et al., 2009a). The animal use protocol was approved by the Animal Subjects Committee from the University of California San Diego. oFPAEC and UAEC were cultured in complete MCDB131 medium (GIBICO) containing 10% fetal calf serum (FCS) and used in passages 8–11 and 4–5, respectively. Human umbilical cord vein endothelial cells (HUVEC) were isolated from healthy term placentas by collagenase digestion as described (Caulin-Glaser et al., 1997). Cords were collected from the University of California Irvine Medical Center Hospital and approved by the Institutional Review Boards. HUVEC were cultured in endothelial cell medium containing 5% fetal bovine serum and supplemented with 1% antibiotics and 1% endothelial cell growth supplement (ScienCell, Carlsbad, CA) and used within five passages. When cells grown to ~80% confluence, the medium was replaced with M199 containing 0.1% BSA, 25mM HEPES overnight. Following 1 h equilibration with fresh M199–0.1% BSA-25 mM HEPES, the cells were treated with VEGF for various times with/without the NOS inhibitor L-NAME or its inactive form D-NAME; drugs were added 1 h before VEGF treatment. Cellular proteins were prepared in a non-denaturing buffer as previously described (Chen et al., 2004). Protein concentration was determined by the BCA Protein Assay Kit (Pierce, Rockford, IL).

siRNA knockdown of eNOS

Endogenous eNOS was knockdown by specific siRNAs as previously described (Zhang et al., 2012). The eNOS-specific siRNA (5'-GAGTTACAAGATCCGCTTCdTdT-3') and a control siRNA (5'-AUUGUAUGCG AUCGCAGACdTdT-3') were synthesized by Dharmacon (Lafayette, CO). Transfection of siRNA was performed with RNAiMAX reagent (Invitrogen, Carlsbad, CA) following the manufacturer's protocol.

Biotin switch technique (BST) and avidin capture

SNO-proteins were labeled with biotin-HPDP by BST as previously described (Zhang et al., 2010). The biotinylated *SNO*-proteins were captured by NeutrAvidin protein coated beads (Thermo scientific, Rockford, IL) at 4°C overnight. The avidin captured proteins were eluted from with 1x SDS sample buffer containing 100 mM 2-mercaptoethenol at 37°C for 20 min and used for immunoblotting.

Liquid chromatography–tandem mass spectrometry (LC-MS/MS) and *SNO*-peptide identification

Proteins were digested by trypsin and the resulting peptides were analyzed by LC-MS/MS as described previously (Wang et al., 2010). LC-MS/MS analysis of *SNO*-peptides was carried out using an LTQ-Orbitrap XL MS (Thermo Scientific, San Jose, CA) coupled with an Eksigent NanoLC system (Eksigent, Dublin, CA). The LC analysis was performed using a capillary column (100 μm ID × 150 mm long) packed with C18 resins (GL Sciences, Torrance, CA) and the peptides were eluted using a linear gradient of 2–40% B in 80 min; (solvent A: 100% H_2O/0.1% formic acid; solvent B: 100% acetonitrile/0.1% formic acid). A cycle of one full Fourier Transform Ion Cyclotron Resonance MS scan mass spectrum (350–1800 *m/z*, resolution of 60,000 at *m/z* 400) was followed by ten data-dependent MS/MS acquired in the linear ion trap with normalized collision energy (setting of 35%). Target ions selected for MS/MS were dynamically excluded for 30 s. Monoisotopic masses of parent ions and corresponding fragment ions, parent ion charge states, and ion intensities from LC-MS/MS spectra were extracted using in-house software based on the Raw-Extract script from Xcalibur version 2.4. The data were searched using the Batch-Tag within the developmental version (v 5.10.0) of Protein Prospector against a decoy database consisting of a normal Swissprot database concatenated with its randomized version (SwissProt.2010.08.10.random.concat). The mass accuracy for parent ions and fragment ions was set as ±20 ppm and 0.6 Da, respectively. Trypsin was set as the enzyme and maximum of two missed cleavages were allowed. Biotin-HPDP labeling of cysteine residues were selected as constant modifications with a monoisotopic mass shift of 428.192 Da.

Site-directed mutagenesis and cell transfection

The pCMV6-Entry shuttle vector carrying the Myc-DDK-tagged human full-length CFL1 cDNA (CFL1/pCMV-Entry vector) was purchased from OriGene Technologies (Rockville, MD). This clone was used to prepare CFL1 mutant constructs in which cysteine was replaced by Ala or Ser by PCR-based site-directed mutagenesis (Hemsley et al., 1989) and confirmed by sequencing; the resulting mutants were named as DMA (C80/139A) and DMS (C80/139S), respectively. A constitutively activated CFL1 mutant (S3A) was also constructed with this clone, in which Ser-3 was replaced by Ala. All the constructs have a Flag-tag at their N-termini. Cell transfection was achieved with GeneJet™ Transfection Reagent (SignaGen Laboratories, Rockville, MD) following the manufacturer's instructions.

Preparation of recombinant CFL1 and its mutant proteins

The pCMV6 vectors containing CFL1 or mutants were transfected into 293T cells. The 293T cells were grown in DMEM medium (Invitrogen, Carlsbad, CA) containing 10% FBS for 48 h. The cells were harvested and sonicated in TBS (50 mM Tris-HCl, pH 7.4, 150 mM NaCl) containing 1 mM EDTA, 1% Triton X-100 and protease inhibitors. Anti-Flag M2 affinity beads (Sigma, St Louis, MO) were added into protein lysates (20 μl resin slurry/10 mg protein), and incubated at 4°C for 2 h. The recombinant Flag-tagged CFL1 and its mutants were pulled down by 3xFlag peptide according to the manufacturer's instructions.

All recombinant proteins displayed as a single band on SDS-PAGE, with an estimated molecular weight of ~26 kDa.

Actin filament severing assay

The activity of recombinant CFL1 and its mutant proteins was measured by the ability of severing in vitro formed F-actin using fluorescence microscopy as previously described (Chan et al., 2000). Briefly, a nitrocellulose-coated flow cell was coated with anti-biotin antibodies (Sigma, St Louis, MO) in ISAP buffer (20 mM Tris-HCl, pH 7.2, 5 mM EGTA, 2 mM $MgCl_2$, 50 mM KCl, 1 mM ATP, 1 mM DTT) by perfusion for 5 min, followed by incubation with ISAP buffer containing 0.5 mg/ml BSA for 5 min. Rhodamine-labeled actin (0.4 μM), biotin-labeled actin (0.2 μM), and unlabeled actin (1.4 μM) were purchased from Cytoskeleton Inc. (Denver, CO) and co-polymerized at room temperature for 2 h in ISAP buffer. The in vitro formed fluorescently labeled F-actin was injected into the anti-biotin antibody coated flow cell with anti-bleaching buffer (ISAP buffer containing 5 mg/ml BSA, 0.036 mg/ml catalase, 0.02 mg/ml glucose oxidase, 6 mg/ml glucose, 100 mM DTT, 1 mM ATP) for 5 min. Unbound F-actin was washed off with anti-bleaching buffer. The assay was initiated by the addition of recombinant CFL1 proteins (1 μM). F-actin deploymerization was observed under an inverted Leica fluorescence microscopy. Images were captured by a Hamamatsu CCD camera using SimplePCI software (Hamamatsu, Bridgewater, NJ) for measuring the length and number of actin filaments by using NIH ImageJ. Actin filaments from five images of each treatment at different incubation times were measured and sub-populated by length > 1 um or ≤ 1 um. Increased number of short actin filament (length ≤ 1 um) and decreased number of long actin filament (length > 1 um) indicate F-actin depolymerization.

Immunoprecipitation, SDS-PAGE, and immunoblotting

Protein lysates were prepared with TBS containing 1 mM EDTA, 1% Triton X-100 and protease inhibitors. Equal amounts of proteins (1 mg) were subjected to immunoprecipitation with 20 μl anti-FLAG M2 affinity beads at 4°C overnight. The Flag-tagged recombinant CFL1 and its mutants were pulled down following the manufacturer's instructions. Protein samples were dissolved in SDS sample buffer and separated by SDS-PAGE and transferred on PVDF membranes and analyzed by immunoblotting (Liao et al., 2009a). The integrated relative densities of bands (proteins) were quantified by multiplying the absorbance of the surface areas by using NIH ImageJ.

F/G-actin ratio

The F/G-actin ratio was determined by an in vivo G-actin/F-actin assay kit (Cytoskeleton, Denver, CO) following the manufacturer's instructions. Briefly, serum-starved cells were treated with/without VEGF (10 ng/ml) for 30 min. The cells were lysed with actin stabilization buffer [50 mM PIPES pH 6.9, 50 mM NaCl, 5 mM $MgCl_2$, 5 mM EGTA, 5% (v/v) glycerol, 0.1% Nonidet P40, 0.1% Triton X-100, 0.1% Tween 20, 0.1% 2-mercaptoethanol, 0.001% antifoam C, 1 mM ATP, and protease inhibitor] and homogenized by using a 25G syringe needle. Lysates were centrifuged at room temperature for 5 min in a tabletop centrifuge at 500 × g to remove unbroken cells and debris, followed by centrifugation at 100,000 x g at 37° C for 1 h. The supernatant containing G-actin was

recovered, and the pellet containing F-actin was solubilized with actin depolymerization buffer (50 mM PIPES, pH 6.9, 50 mM NaCl, 5 mM $MgCl_2$, and 10 μM cytochalasin D). Aliquots of both fractions were separated on SDS-PAGE and then blotted with anti-actin antibody (Sigma, St Louis, MO). The band densities of F/G-actin were quantified for calculating the cellular F/G-actin ratio.

Immunofluorescence staining of F-actin and Flag-CFL1

oFPAEC were grown on glass coverslips and transfected with flag-tagged wt-CFL1 or its mutant plasmids. After treatment with VEGF, the cells were fixed for immunofluorescence staining as described previously (Liao et al., 2009b), with TRITC-labeled anti-phalloidin to visualize F-actin (red) and with an FITC-labeled anti-Flag antibody (Sigma–Alderich) to visualize Flag-CFL1 (green). Relative immunofluorescence intensities were quantified by using SimplePCI software.

Cell migration assay

Cell migration was determined by a scratch wound assay as described previously (Liao et al., 2009b) with modifications as below. Briefly, oFPAEC were transfected with wild-type (wt-) CFL1 or its mutant plasmids and grown on collegan-coated glass coverslips. Confluent oFPAEC monolayer was scrapped by using a sterilized 200 μl pipette tip. After wounding, the cells were washed with serum-free M199 medium and cultured in M-199 containing 0.1% BSA and 1%FCS with/without VEGF for 24 h. The cells were fixed for immunofluorescence staining with TRITC-labeled anti-phalloidin and the FITC-labeled anti-Flag antibody as described above. The distance of the cells moved from the wounding edge toward the center of the wound was measured and averaged as an index for cell migration. Non-transfected cells in the same slide served as the control.

Filopodium formation

oFPAEC were seeded on glass coverslips and grew to ~70% confluence. Following transfection and VEGF treatment, cells were fixed with 4% formaldehyde in Ca^{2+}/Mg^{2+}-free PBS and washed with Ca^{2+}/Mg^{2+}-free PBS containing 0.1% Triton X-100. The fixed cells were stained with TRITC-phalloidin to visualize F-actin under a Leica fluorescence microscopy for image acquisition by a Hamamatsu high-resolution CCD camera using SimplePCI. Protrusions that contain actin with a width of 0.6–1.2 μm and an average length between 6 and 15 μm were defined as filopodia (Lim et al., 2008). The filopodium number of 30 cells per treatment was counted and averaged for statistical comparison among different groups.

Experimental replication and statistical analysis

All experiments were repeated at least three times using cells from different subjects. Data were presented as mean ± SEM. Statistical analysis was performed by one-way ANOVA, followed by Student–Newman–Keuls test for multiple comparisons. Significant difference was defined as $P < 0.05$.

Results

VEGF rapidly induces S-nitrosylation of CFL1 in endothelial cells

Treatment with VEGF stimulated S-nitrosylation of CFL1 in a time-dependent manner in oFPAEC. Following treatment with VEGF, *SNO*-CFL1 level increased significantly at 15 min and maximized at 30 min, and then returned to baseline at 60 min. Treatment with a NO donor GSNO also stimulated S-nitrosylation of CFL1 time-dependently but with a different time-course; the response began in 15 min, maximized at 30 min, and maintained at high levels up to 60 min (Fig. 1a). Similar to oFPAEC, treatment with VEGF also significantly stimulated S-nitrosylation of CFL1 in UAEC and HUVEC at 30 min (Fig. 1b), demonstrating that VEGF induces S-nitrosylation of CFL1 in different endothelial cells.

VEGF stimulation of S-nitrosylation of CFL1 is mediated by eNOS-derived NO

Pretreatment with a NOS inhibitor L-NAME, but not its inactive form D-LAME, blocked VEGF-induced S-nitrosylation of CFL1 in all three types of endothelial cells (Fig. 1b). When eNOS was knocked down by using eNOS-specific small interfering RNAs (siRNAs), the VEGF-stimulated S-nitrosylation of CFL1 was blocked in oFPAEC (Fig. 1c). As a control, treatment with scramble siRNAs did not affect VEGF-stimulated S-nitrosylation of CFL1. Thus, these findings demonstrate that eNOS-derived NO mediates VEGF stimulation of S-nitrosylation of CFL1 in endothelial cells.

Cys-80 and Cys-139 are the major *SNO*-sites in CFL1

Identification of specific *SNO*-site(s) in target proteins is required for functional analysis of S-nitrosylation as S-nitrosylation only occurs on specific cysteines (Hess et al., 2005). With biotin switch technique, we labeled the *SNO*-modified cysteines in CFL1 with *Biotin*-HPDP for analyzing the specific SNO-sites in CFL1 by LC-MS/MS. We identified peptides with *m/z* of 713.991 (MH_3^{3+}) and 945.932 (MH_3^{2+}), corresponding to the expected *m/z* values of *Biotin*-HPDP modified DC_{80}RYALYDATYETK and HELQANC$_{139}$ YEEVK, respectively. MS/MS analysis of these two peptides confirmed that Cys-80 and Cys-139 were labeled with biotin-HPDP, indicating these two sites as the *SNO*-modified sites among the four cysteines (Cys-39/80/139/147) in CFL1 (Fig. 2a).

We then constructed two CFL1 mutants, that is, DMA and DMS, by replacing Cys-80/139 with Ala or Ser, respectively. The wt-CFL1 and its mutant DMA and DMS were overexpressed in 293T cells. The cell lysates were incubated with/without 1 mM GSNO at 37°C for 30 min. After GSNO removal with Amicon centrifugal filters (Millipore, Billerica, MA), total biotin-labeled *SNO*-proteins were captured by avidin coated beads for determining *SNO*-CFL1 by immunoblotting with an anti-CFL1 antibody. Basal *SNO*-CFL1 was barely detected in all samples. Treatment with GSNO dramatically increased S-nitrosylation of wt-CFL1. Compared to wt-CFL1, S-nitrosylation of DMA and DMS were barely detectable with/without GSNO treatment. SNO-β-actin was detectable and similarly enhanced by GSNO in all samples (Fig. 2b). These data show that C80/139A/S mutations prevent S-nitrosylation of CFL1, further confirming Cys-80 and Cys-139 as the major SNO sites in CFL1.

S-nitrosylation enhances the actin filament severing activity of CFL1

We compared the activities of recombinant wt-, DMA, and DMS CFL1 proteins by using an in vitro actin filament severing assay; in this assay, a constitutively active CFL1 mutant S3A (replacing Ser3 with Ala) (Yang et al., 1998) was used as positive control. When no recombinant CFL1 proteins were added, both length and number of the fluorescently labeled F-actin fibers were unchanged over time. Incubation with wt-CFL1 protein significantly deploymerized F-actin as evidenced by reduced number and length of F-actin. Compared to wt-CFL1, incubation with DMA-CFL1 further decreased both number and length of F-actin; whereas incubation with DMS-CFL1 did not change the number and length of F-actin. As a positive control, the S3A mutant protein showed the highest activity in severing F-actin (Fig. 3). Because replacement of *SNO*-cysteines with Ala exerts a SNO-mimetic effect, and with Ser exerts a *SNO*-deficient effect (McMahon et al., 2000; Hara et al., 2005; Huang et al., 2005; McMahon et al., 2002; Ozawa et al., 2008), recombinant DMA and DMS CFL1 proteins functioned as *SNO*-mimetic and *SNO*-deficient CFL1, respectively. Thus, our findings show that S-nitrosylation of CFL1 enhances its F-actin severing activity.

S-nitrosylation decreases CFL1 phosphorylation

We tested if S-nitrosylation affects Ser-3 phosphorylation of CFL1 because the function of CFL1 is known to be regulated by Ser-3 phosphorylation, with phosphorylated form to be inactive (Moriyama et al., 1996). When transfected in oFPAEC, treatment with VEGF for 15 min significantly stimulated S-nitrosylation of flag-tagged wt-CFL1, but not DMA or DMS CFL1s, confirming that Cys-80/139 were the major functional *SNO*-sites in CFL1. High basal Ser-3 phosphorylation was detected in the wt-CFL1, which was significantly reduced by VEGF stimulation. Ser-3 phosphorylation of DMA CFL1 was barely detectable with/without VEGF treatment. DMS CFL1 was phosphorylated under basal condition; the level was significantly lower than that of wt-CFL1 and was also unresponsive to VEGF (Fig. 4a). Thus, these findings suggest that regulation of CFL1 function via S-nitrosylation may be related to Ser-3 phosphorylation.

S-nitrosylation enhances CFL1 binding to actin

Since binding to actin is a critical step for CFL1 to elicit its actin-severing activity (Condeelis, 2001), we measured the in vivo actin-binding ability of recombinant CFL1 proteins. When overexpressed in oFPAEC, wt-CFL1 did not bind actin in resting condition. However, treatment with VEGF for 30 min dramatically increased the level of actin bound wt-CFL1. In comparison to wt-CFL1, the level of actin bound DMA-CFL1 was similar to that of VEGF-induced actin bound wt-CFL1, but this level was unaltered by VEGF. Basal level of actin bound DMS-CFL1 was detectable but low and also unresponsive to VEGF treatment. As expected, flag-tagged CFL1s was undetectable in the vector-transfected controls (Fig. 4b). These data suggest that S-nitrosylation of CFL1 on Cys-80/139 may have maximized its actin-binding activity and S-nitrosylation may be a major mechanism responsible for increasing the actin-binding activity of CFL1 upon VEGF stimulation.

SNO-CFL1 regulates F-actin formation in endothelial cells

We next investigated the effects of *SNO*-CFL1 on VEGF-induced F-actin formation in oFPAEC overexpressing wt-CFL1 and its mutants. The flag-tagged CFL1s and F-actin were labeled with red and green fluorescence in the cells, respectively. Non-transfected cells that were not labeled with green fluorescence were used as controls in each group. Basal levels of F-actin in the cells overexpressing wt-CFL1 were significantly lower than that in non-transfected control cells. Compared to wt-CFL1, S3A and DMA mutants further decreased basal F-actin levels; whereas the DMS mutant was ineffective. VEGF stimulated F-actin formation in non-transfected cells and overexpression of wt-CFL1 decreased this response. However, VEGF did not alter F-actin levels in cells overexpressing S3A, DMA or DMS mutants (Figs. 5a and b).

We further measured F/G actin ratio to determine the effects of CFL1 and its mutants on F-actin formation in oFPAEC. In non-transfected cells, treatment with VEGF significantly increased F/G actin ratio, consistent with our recent report showing the stimulatory effects of VEGF on F-actin formation (Liao et al., 2009b). Overexpression of the constitutively active S3A CFL1, but not wt- or DMA/DMS CFL1s, decreased basal F/G-actin ratio. Overexpression of wt-CFL1, but not the S3A or DMA mutants, significantly inhibited VEGF-induced F-actin formation, resulting in lower F/G-actin ratio in VEGF-treated cells than baseline. However, VEGF was still able to increase the F/G-actin ratio in cells overexpressing DMS CFL1 (Fig. 5c).

These findings show that once the regulatory sites Cys-80/139 and Ser-3 are mutated, VEGF is unable to regulate F-actin formation via CFL1, implicating that CFL1 regulates F-actin formation in endothelial cells via both S-nitrosylation and phosphorylation.

SNO-CFL1 regulates VEGF-induced endothelial migration

We then investigated the effects of *SNO*-CFL1 on VEGF stimulation of oFPAEC migration by using a scratch wound assay with cells that were overexpressed with wt-CFL1 and its mutants. In this assay, F-actin and flag-tagged CFL1 were labeled with red and green fluorescence in the cells, respectively. Non-transfected cells without green fluorescence labeling in each group were used as controls. The distance of cell migration with/without VEGF stimulation was measured as an index for cell migration. As expected, VEGF significantly stimulated cell migration. Overexpression of wt-CFL1 suppressed the VEGF-induced cell migration. In comparison to the wt-CFL1, S3A and DMA mutants further decreased the VEGF-induced cell migration, whereas the DMS mutant had no effects (Fig. 6). These findings show that CFL1 regulates VEGF-induced endothelial cell migration via S-nitrosylation on Cys-80/139 and Ser-3 phosphorylation.

SNO-CFL1 regulates filopodium formation in endothelial cells

Cell migration initiates with filopodium formation at the leading edges of a cell (Lauffenburger and Horwitz, 1996). We then determined if filopodium formation is involved in VEGF-induced endothelial cell migration via S-nitrosylation of CFL1. Overexpression of wt-CFL1 significantly decreased basal number of filopodia (arrows, Fig. 7) per cell in oFPAEC. This number was further decreased in oFPAEC overexpressing S3A and DMA

mutants; whereas the DMS mutant had no effects. Treatment with VEGF significantly increased filopodium formation in non-transfected and DMS-transfected oFPAEC. However, VEGF was unable to stimulate filopodium formation in cells overexpressing wt-CFL, S3A or DMA (Fig.7). These findings show that once Cys-80/139 and Ser-3 are mutated, VEGF is unable to regulate filipodium formation via CFL1. These data show that both S-nitrosylation and phosphorylation of CFL1 are involved in the regulation of filipodium formation in endothelial cells (Fig. 8).

Discussion

By using proteomics approaches, we and other groups have recently identified CFL1 as a major *SNO*-protein in endothelial cells (Dall'Agnol et al., 2006; Han and Chen, 2008; Zhang et al., 2010, 2012), raising a question whether S-nitrosylation regulates CFL1 function as related to endothelial cell actin dynamics, migration, and angiogenesis. In this study, we tested whether S-nitrosylation of CFL1 regulates its function and endothelial actin cytoskeleton remodeling and migration in response to VEGF stimulation. We have shown herein that VEGF stimulates S-nitrosylation of CFL1 in endothelial cells in a time-dependent manner via endogenous NO derived from eNOS because: (1) NOS inhibition with L-NAME significantly suppressed VEGF-stimulated S-nitrosylation of CFL1; and (2) VEGF fails to stimulate S-nitrosylation of CFL1 in endothelial cells in which eNOS is knocked down by the eNOS-specific siRNA. We have previously demonstrated that endogenous NO is one of the essential mediators for VEGF-induced endothelial cell migration (Liao et al., 2009b). Therefore, S-nitrosylation of CFL1 provides an important mechanism by which endogenous NO regulates endothelial cell migration upon VEGF stimulation.

We have observed that the time-course of S-nitrosylation response to endogenous NO via eNOS by VEGF stimulation is quite different from that of exogenous NO from GSNO. Both induce maximal *SNO*-CFL1 at 30 min; however, the VEGF-induced response returns to baseline at 60 min, while GSNO-induced did not. These findings suggest that VEGF stimulation of *SNO*-CFL1 is a regulatory physiological process in endothelial cells. Although our current study cannot explain why longer VEGF treatment *de*-nitrosylates *SNO*-CFL1, the underlying mechanisms are likely associated with activation of enzymes for denitrosylating *SNO*-proteins, such as S-nitrosoglutathione reductase (Lima et al., 2009) and thioredoxin reductase (Benhar et al., 2010) that are key enzymes for S-nitrosylation homeostasis.

Although S-nitrosylation has been identified as a crucial mechanism by which NO regulates protein functions directly, the fragile S-NO bond can be accurately measured until BST was invented in 2001 (Jaffrey and Snyder, 2001); this method has now been accepted as the most reliable approach for SNO measurement (Jaffrey and Snyder, 2001; Derakhshan et al., 2007; Wang et al., 2008; Foster et al., 2009; Chouchani et al., 2010). In this method, SNO groups are selectively reduced by ascorbate and then labeled with biotin, thus allowing nitrosoproteins to be readily displayed, affinity purified and identified. Similar to *O*-phosphorylation and other *post*-translational modifications that occur on specific residues, S-nitrosylation occurs only on certain specific cysteines (Hess et al., 2005). By using BST-based mass spectrometry and with further verification by point mutation

studies, we have identified Cys-80 and Cys-139 to be the major *SNO*-sites among the 4 cysteines (39/80/139/147) in CFL1. When Cys-80 and Cys-139 are replaced with Ala or Ser, GSNO-induced *SNO*-CFL1 in vitro (Fig. 2b) and VEGF-induced *SNO*-CFL1 in endothelial cells (Fig. 3) are greatly reduced. We also observe that *SNO*-CFL1 were still detectable even when both Cys-80/139 were mutated. However, the very low S-nitrosylation response stimulated with 1 mM GSNO on the other two cysteines (39/147) might be irrelevant.

Because S-nitrosylation increases local hydrophobicity, substitution with relatively hydrophobic residues exerts a *SNO*-mimetic effect (Ozawa et al., 2008), Cys→Ala/Ser mutation on *SNO*-sites has been used as a tool for characterizing *SNO*-mimetic/deficient effect (McMahon et al., 2000, 2002; Hara et al., 2005; Huang et al., 2005; Ozawa et al., 2008). We have used the Cys-80/139 Ala/Ser mutants for determining the functional significance of S-nitrosylation of CFL1. First, we found that S-nitrosylation results in significantly increased actin binding/severing activity of recombinant CFL1 protein in vitro. Recombinant *SNO*-mimetic Cys-80/139→Ala (DMA) mutant protein possesses greater capacity of depolymerizing in vitro formed F-actin than that of the wt-CFL1 protein; whereas the Cys-80/139→Ser (DMS) mutant protein seems to have reduced activity. When these mutants were overexpressed in endothelial cells, VEGF treatment is only able to nitrosylate wt-CFL1, but not DMA or DMS. In DMA-CFL1 transfected cells, the level of CFL1 bound actin is significantly greater than that in cells transfected with wt-CFL1 and DMS. Consistently, F-actin and F/G-actin ratio in endothelial cells are significantly decreased in cells transfected with wt- or DMA, but not DMS, CFL1s. Moreover, VEGF treatment is able to increase the actin-binding activity of wt-CFL1, but not DMA, suggesting that S-nitrosylation may have maximized the actin binding capacity of CFL1.

The function of CFL1 is known to be regulated by phosphorylation/dephosphorylation on Ser-3 via a so-called cofilin pathway comprising multiple kinases and phosphatases, with phosphorylated form to be inactive (Moriyama et al., 1996; Arber et al., 1998; Toshima et al., 2001; Niwa et al., 2002; Gohla et al., 2005). Our findings suggest that the mechanisms by which S-nitrosylation increase the actin-binding activity of CFL1 is likely related to phosphorylation due to the following reasons. When overexpressed in endothelial cells, wt-CFL1 is readily phosphorylated and VEGF dephosphorylates it; in contrast, basal phosphorylation of DMA, the *SNO*-mimic CFL1 mutant, is barely detectable and VEGF is unable to alter its phosphorylation. In addition, basal phosphorylation of DMS, the *SNO*-deficient CFL1 mutant, is significantly lower than that of wt-CFL1; VEGF also does not alter its phosphorylation. Interestingly, we have observed that replacing Cys-80/139 with Ala decreases Ser-3 phosphorylation of CFL1. This phenomenon is likely due to protein conformational changes caused by the mutations, preventing Ser-3 from phosphorylation by protein kinases (Niwa et al., 2002; Kobayashi et al., 2006). This may represent a mechanism for increasing the actin-binding/severing activity of CFL1 via S-nitrosylation.

Cell migration initiates when a cell senses extracellular stimuli; the cell then sends out protrusions (fillopodia and lamellipodia) at the leading edge, assembling focal adhesion for attachment and forms stress fiber for contraction; finally, its rear is released to complete a migrating cycle (Mattila and Lappalainen, 2008). VEGF is well-known to stimulate endothelial cell migration (Ferrara et al., 2003). We have previously demonstrated that

endogenous NO mediates VEGF-induced endothelial cell migration (Liao et al., 2009b). Our current data suggest that overexpression of wt-CFL1, S3A, and DMA mutants significantly inhibit VEGF-stimulated endothelial cell migration. In comparison, the constitutive active S3A mutant has the greatest ability in suppressing endothelial cell migration and DMA mutant is comparably effective, followed by the wt-CFL1; whereas the DMS mutant has little effect. These findings are consistent with the function of active CFL1 in severing/depolymerizing F-actin (Andrianantoandro and Pollard, 2006). Thus, both S-nitrosylation on Cys-80/139 and phosphorylation on Ser-3 are important for VEGF activation of CFL1. We also have found that overexpression of active CFL1 (S3A/DMA) inhibits basal filopodium formation; whereas the inactive CFL1 does not. Moreover, wt-CFL1 and the S3A and DMA mutants have comparably inhibitory effects on the VEGF-stimulated filopodium formation. These data demonstrate that the effects of CFL1 on VEGF-induced endothelial cell migration occur at the early stage of cell migration by affecting filopodium formation via both S-nitrosylation and phosphorylation dependent mechanisms.

Altogether, our current study have shown that VEGF stimulates dynamic S-nitrosylation of CFL1 via eNOS-derived NO, resulting in increased actin severing activity of CFL1 for regulating actin dynamics and cytoskeleton remodeling as well as migration in endothelial cells. Thus, our current study has defined a novel pathway *post*-NO biosynthesis for VEGF stimulation of endothelial cell migration. We believe this mechanism has important implications in biology and medicine because actin dynamics and cytoskeleton remodeling as well as migration are fundamental cellular processes that are involved in all physiological processes such as angiogenesis and pathological processes such as tumor growth and metastasis (Carmeliet and Jain, 2000).

Acknowledgments

This study was supported in part by the National Institutes of Health grants R21 HL98746, RO1 HL74947 & RO1 HL70562 (to DB Chen), RO1 GM74830 & R21 CA161807 (to L Huang) and American Heart Association grant SDG13910006 (to HH Zhang).

Literature Cited

Andrianantoandro E, Pollard TD. 2006. Mechanism of actin filament turnover by severing and nucleation at different concentrations of ADF/cofilin. Mol Cell 24:13–23. [PubMed: 17018289]

Arber S, Barbayannis FA, Hanser H, Schneider C, Stanyon CA, Bernard O, Caroni P. 1998. Regulation of actin dynamics through phosphorylation of cofilin by LIM-kinase. Nature 393:805–809. [PubMed: 9655397]

Arnold WP, Mittal CK, Katsuki S, Murad F. 1977. Nitric oxide activates guanylate cyclase and increases guanosine 3':5'-cyclic monophosphate levels in various tissue preparations. Proc Natl Acad Sci U S A 74:3203–3207. [PubMed: 20623]

Bartlett GJ, Porter CT, Borkakoti N, Thornton JM. 2002. Analysis of catalytic residues in enzyme active sites. J Mol Biol 324:105–121. [PubMed: 12421562]

Benhar M, Thompson JW, Moseley MA, Stamler JS. 2010. Identification of S-nitrosylated targets of thioredoxin using a quantitative proteomic approach. Biochemistry 49:6963–6969. [PubMed: 20695533]

Carmeliet P, Jain RK. 2000. Angiogenesis in cancer and other diseases. Nature 407:249–257. [PubMed: 11001068]

Caulin-Glaser T, Garcia-Cardena G, Sarrel P, Sessa WC, Bender JR. 1997. 17 beta-estradiol regulation of human endothelial cell basal nitric oxide release, independent of cytosolic Ca2+ mobilization. Circ Res 81:885–892. [PubMed: 9351464]

Chan AY, Bailly M, Zebda N, Segall JE, Condeelis JS. 2000. Role of cofilin in epidermal growth factor-stimulated actin polymerization and lamellipod protrusion. J Cell Biol 148:531–542. [PubMed: 10662778]

Chen DB, Bird IM, Zheng J, Magness RR. 2004. Membrane estrogen receptor-dependent extracellular signal-regulated kinase pathway mediates acute activation of endothelial nitric oxide synthase by estrogen in uterine artery endothelial cells. Endocrinology 145:113–125. [PubMed: 14512434]

Chen DB, Zhen J. 2014. Regulation of placental angiogenesis. Microcirculation 21:15–25. [PubMed: 23981199]

Chouchani ET, Hurd TR, Nadtochiy SM, Brookes PS, Fearnley IM, Lilley KS, Smith RA, Murphy MP. 2010. Identification of S-nitrosated mitochondrial proteins by S-nitrosothiol difference in gel electrophoresis (SNO-DIGE): Implications for the regulation of mitochondrial function by reversible S-nitrosation. Biochem J 430:49–59. [PubMed: 20533907]

Chrzanowska-Wodnicka M, Kraus AE, Gale D, White GC 2nd, Vansluys J. 2008. Defective angiogenesis, endothelial migration, proliferation, and MAPK signaling in Rap1b-deficient mice. Blood 111:2647–2656. [PubMed: 17993608]

Condeelis J 2001. How is actin polymerization nucleated in vivo. Trends Cell Biol 11:288–293. [PubMed: 11413039]

Dall'Agnol M, Bernstein C, Bernstein H, Garewal H, Payne CM. 2006. Identification of S-nitrosylated proteins after chronic exposure of colon epithelial cells to deoxycholate. Proteomics 6:1654–1662. [PubMed: 16404723]

Derakhshan B, Wille PC, Gross SS. 2007. Unbiased identification of cysteine S-nitrosylation sites on proteins. Nat Protoc 2:1685–1691. [PubMed: 17641633]

Ferrara N, Gerber HP, LeCouter J. 2003. The biology of VEGF and its receptors. Nat Med 9:669–676. [PubMed: 12778165]

Foster MW, Forrester MT, Stamler JS. 2009. A protein microarray-based analysis of S-nitrosylation. Proc Natl Acad Sci U S A 106:18948–18953. [PubMed: 19864628]

Gohla A, Birkenfeld J, Bokoch GM. 2005. Chronophin, a novel HAD-type serine protein phosphatase, regulates cofilin-dependent actin dynamics. Nat Cell Biol 7:21–29. [PubMed: 15580268]

Han P, Chen C. 2008. Detergent-free biotin switch combined with liquid chromatography/tandem mass spectrometry in the analysis of S-nitrosylated proteins. Rapid Commun Mass Spectrom 22:1137–1145. [PubMed: 18335467]

Hara MR, Agrawal N, Kim SF, Cascio MB, Fujimuro M, Ozeki Y, Takahashi M, Cheah JH, Tankou SK, Hester LD, Ferris CD, Hayward SD, Snyder SH, Sawa A. 2005. S-nitrosylated GAPDH initiates apoptotic cell death by nuclear translocation following Siah1 binding. Nat Cell Biol 7:665–674. [PubMed: 15951807]

Hemsley A, Arnheim N, Toney MD, Cortopassi G, Galas DJ. 1989. A simple method for site-directed mutagenesis using the polymerase chain reaction. Nucleic Acids Res 17: 6545–6551. [PubMed: 2674899]

Hess DT, Matsumoto A, Kim SO, Marshall HE, Stamler JS. 2005. Protein S-nitrosylation: Purview and parameters. Nat Rev Mol Cell Biol 6:150–166. [PubMed: 15688001]

Huang Y, Man HY, Sekine-Aizawa Y, Han Y, Juluri K, Luo H, Cheah J, Lowenstein C, Huganir RL, Snyder SH. 2005. S-nitrosylation of N-ethylmaleimide sensitive factor mediates surface expression of AMPA receptors. Neuron 46:533–540. [PubMed: 15944123]

Jaffrey SR, Snyder SH. 2001. The biotin switch method for the detection of S-nitrosylated proteins. Sci STKE 2001:PL1.

Kobayashi M, Nishita M, Mishima T, Ohashi K, Mizuno K. 2006. MAPKAPK-2-mediated LIM-kinase activation is critical for VEGF-induced actin remodeling and cell migration. EMBO J 25:713–726. [PubMed: 16456544]

Krause BJ, Hanson MA, Casanello P. 2011. Role of nitric oxide in placental vascular development and function. Placenta 32:797–805. [PubMed: 21798594]

Lamalice L, Le Boeuf F, Huot J. 2007. Endothelial cell migration during angiogenesis. Circ Res 100:782–794. [PubMed: 17395884]

Lauffenburger DA, Horwitz AF. 1996. Cell migration: A physically integrated molecular process. Cell 84:359–369. [PubMed: 8608589]

Liao WX, Feng L, Zhang H, Zheng J, Moore TR, Chen DB. 2009a. Compartmentalizing VEGF-induced ERK2/1 signaling in placental artery endothelial cell caveolae: A paradoxical role of caveolin-1 in placental angiogenesis in vitro. Mol Endocrinol 23:1428–1444. [PubMed: 19477952]

Liao WX, Feng L, Zheng J, Chen DB. 2009b. Deciphering mechanisms controlling placental artery endothelial cell migration stimulated by vascular endothelial growth factor. Endocrinology 151:3432–3444.

Lim KB, Bu W, Goh WI, Koh E, Ong SH, Pawson T, Sudhaharan T, Ahmed S. 2008. The Cdc42 effector IRSp53 generates filopodia by coupling membrane protrusion with actin dynamics. J Biol Chem 283:20454–20472. [PubMed: 18448434]

Lima B, Lam GK, Xie L, Diesen DL, Villamizar N, Nienaber J, Messina E, Bowles D, Kontos CD, Hare JM, Stamler JS, Rockman HA. 2009. Endogenous S-nitrosothiols protect against myocardial injury. Proc Natl Acad Sci USA 106:6297–6302. [PubMed: 19325130]

Mattila PK, Lappalainen P. 2008. Filopodia: Molecular architecture and cellular functions. Nat Rev Mol Cell Biol 9:446–454. [PubMed: 18464790]

McMahon TJ, Stone Exton, Bonaventura A, Singel J, Solomon DJ, Stamler. 2000. Functional coupling of oxygen binding and vasoactivity in S-nitrosohemoglobin. J Biol Chem 275:16738–16745. [PubMed: 10747928]

McMahon TJ, Moon RE, Luschinger BP, Carraway MS, Stone AE, Stolp BW, Gow AJ, Pawloski JR, Watke P, Singel DJ, Piantadosi CA, Stamler JS. 2002. Nitric oxide in the human respiratory cycle. Nat Med 8:711–717. [PubMed: 12042776]

Moriyama K, Iida K, Yahara I. 1996. Phosphorylation of Ser-3 of cofilin regulates its essential function on actin. Genes Cells 1:73–86. [PubMed: 9078368]

Niwa R, Nagata-Ohashi K, Takeichi M, Mizuno K, Uemura T. 2002. Control of actin reorganization by Slingshot, a family of phosphatases that dephosphorylate ADF/cofilin. Cell 108:233–246. [PubMed: 11832213]

Ozawa K, Whalen EJ, Nelson CD, Mu Y, Hess DT, Lefkowitz RJ, Stamler JS. 2008. S-nitrosylation of beta-arrestin regulates beta-adrenergic receptor trafficking. Mol Cell 31:395–405. [PubMed: 18691971]

Stupack DG, Cho SY, Klemke RL. 2000. Molecular signaling mechanisms of cell migration and invasion. Immunol Res 21:83–88. [PubMed: 10852105]

Thachil J 2011. Nitric oxide and adverse events of vascular endothelial growth factor inhibitors. Curr Med Res Opin 27:1503–1507. [PubMed: 21651424]

Theriot JA. 1997. Accelerating on a treadmill: ADF/cofilin promotes rapid actin filament turnover in the dynamic cytoskeleton. J Cell Biol 136:1165–1168. [PubMed: 9087434]

Toshima J, Toshima JY, Amano T, Yang N, Narumiya S, Mizuno K. 2001. Cofilin phosphorylation by protein kinase testicular protein kinase 1 and its role in integrin-mediated actin reorganization and focal adhesion formation. Mol Biol Cell 12: 1131–1145. [PubMed: 11294912]

Vicente-Manzanares M, Horwitz AR. 2011. Cell migration: An overview. Methods Mol Biol 769:1–24. [PubMed: 21748665]

Wang X, Kettenhofen NJ, Shiva S, Hogg N, Gladwin MT. 2008. Copper dependence of the biotin switch assay: Modified assay for measuring cellular and blood nitrosated proteins. Free Radic Biol Med 44:1362–1372. [PubMed: 18211831]

Wang X, Yen J, Kaiser P, Huang L. 2010. Regulation of the 26S proteasome complex during oxidative stress. Sci Signal 3:ra88. [PubMed: 21139140]

Yang N, Higuchi O, Ohashi K, Nagata K, Wada A, Kangawa K, Nishida E, Mizuno K. 1998. Cofilin phosphorylation by LIM-kinase 1 and its role in Rac-mediated actin reorganization. Nature 393:809–812. [PubMed: 9655398]

Zhang HH, Feng L, Livnat I, Hoh JK, Shim JY, Liao WX, Chen DB. 2010. Estradiol-17{beta} stimulates specific receptor and endogenous nitric oxide-dependent dynamic endothelial protein

S-nitrosylation: Analysis of endothelial nitrosyl-proteome. Endocrinology 151:3874–3887. [PubMed: 20519370]

Zhang HH, Feng L, Wang W, Magness RR, Chen DB. 2012. Estrogen-responsive nitroso-proteome in uterine artery endothelial cells: Role of endothelial nitric oxide synthase and estrogen receptor-beta. J Cell Physiol 227:146–159. [PubMed: 21374595]

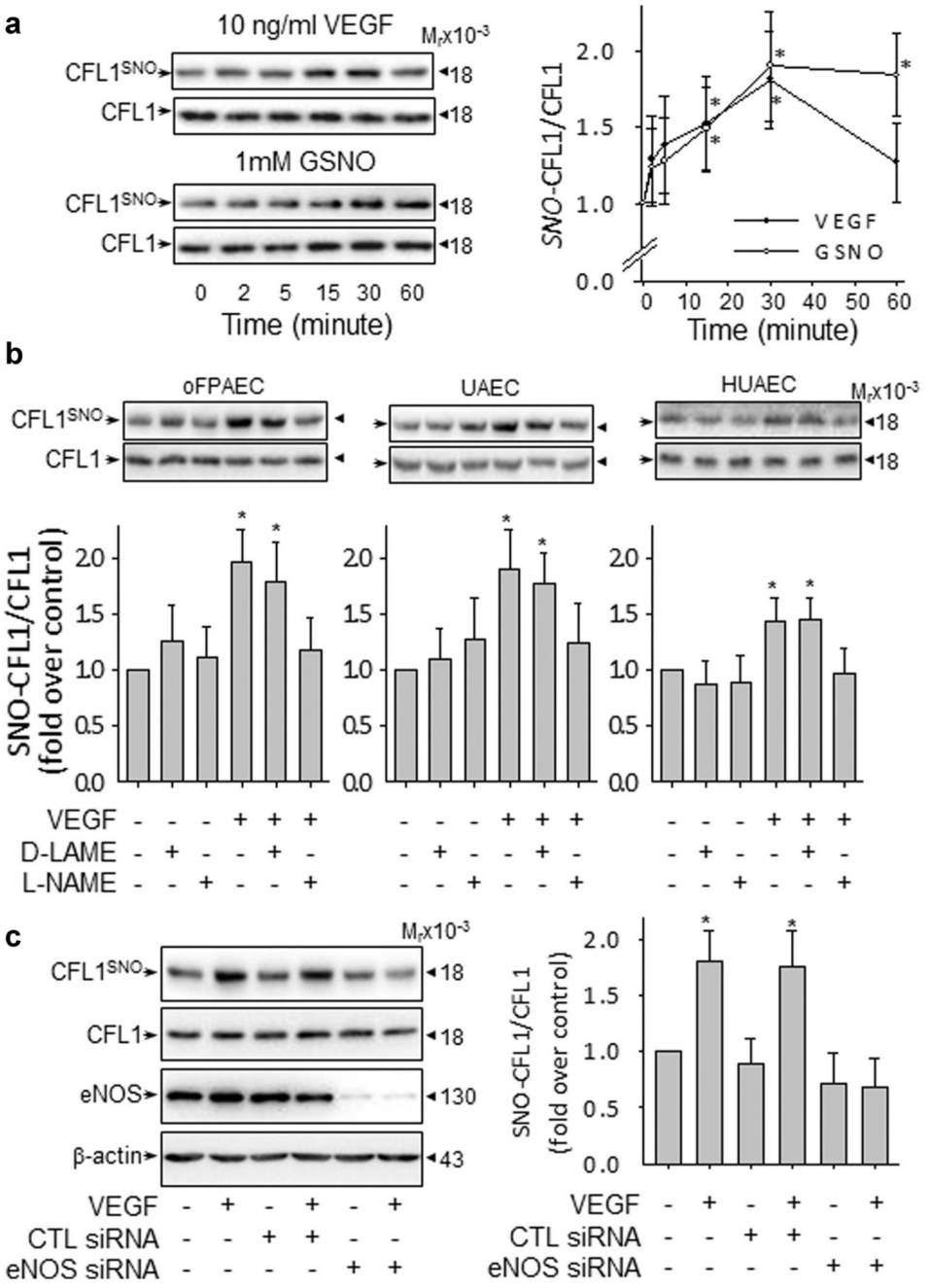

Fig. 1.

VEGF rapidly induces S-nitrosylation of cofilin-1 in endothelial cells via eNOS-derived NO. (a) oFPAEC were treated with 10 ng/ml VEGF or 1mM GSNO for the indicated times. (b) oFPAEC, HUVEC, and UAEC were treated with 10 ng/ml VEGF with/without 1mM L-NAME or D-NAME for 30 min. Total protein extracts were harvested and subjected to biotin-switch. The biotin-labeled *SNO*-proteins were pulled down with avidin capture and analyzed by immunoblotting with anti-CFL1 antibodies to detect *SNO*-CFL1. Blots of *SNO*-CFL1 and total CFL1 (loading control) of one representative experiment are shown. (c) oFAPEC transfected with/without scramble or specific eNOS siRNAs were treated with/

without 10 ng/ml VEGF for 30 min. SNO-CFL1 was measured. Blots of SNO-CFL1, total CFL1, eNOS, and β-actin of one representative experiment are shown. Graphs summarize data (mean ± SEM) from three independent experiments using cells from different pregnant ewes. Data were normalized and expressed fold to control. * $P < 0.05$ versus untreated control.

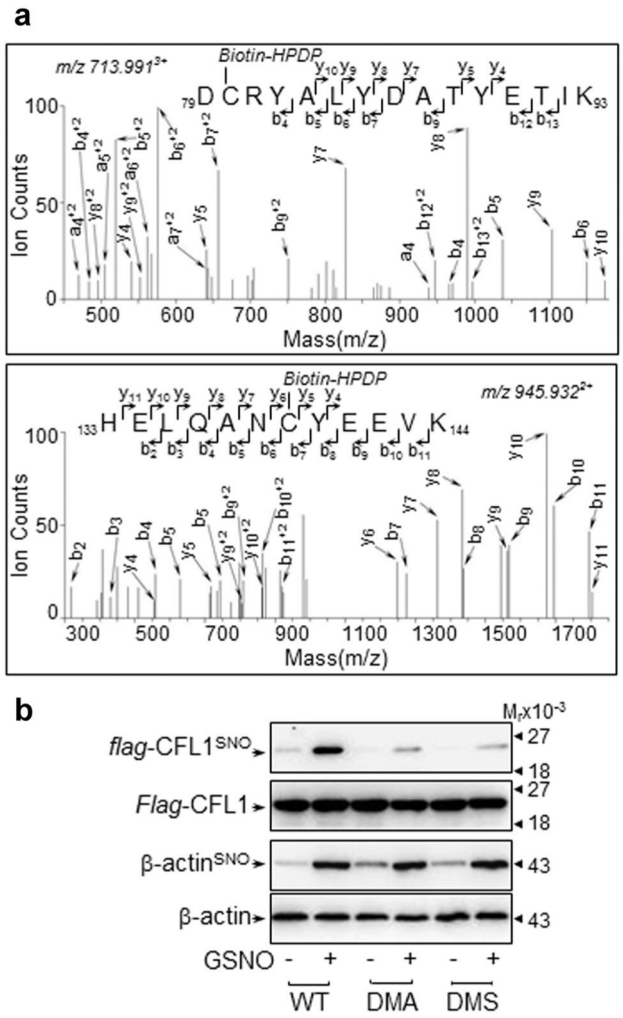

Fig. 2.

Cys80 and Cys139 are identified as major *SNO*-sites in cofilin-1. (a) MS/MS spectra of two peptides with *m/z* of 713.991 (MH_3^{3+}) and 945.932 (MH_2^{2+}). Detection of a series of y and b ions in both MS/MS spectra determined their sequences unambiguously as DC*$_{80}$RYALYDATYETK and HELQANC*$_{139}$ YEEVKR, in which C* is Biotin-HPDP-modified. (b) Flag-tagged wild-type (wt) CFL1 and its DMA or DMS mutants were overexpressed in 293T cells. Whole cell lysates were collected and treated with 1mM GSNO at 37°C for 30 min. The biotin-labeled total SNO-proteins from equal amounts of proteins were avidin captured for analyzing *SNO*-flag-CFL1 and total flag-CFL1 by immunoblotting with an anti-Flag antibody. *SNO*-β-Actin and total β-Actin were used as a positive control. Blots shown represent one of three similar transfection experiments.

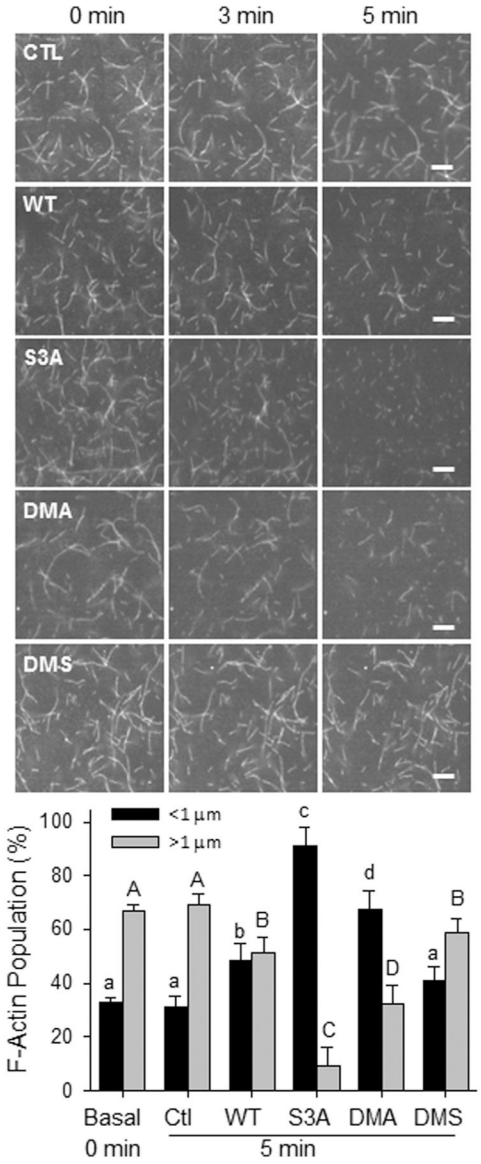

Fig. 3.

Effects of *SNO*-mimetic/deficiency on in vitro actin severing activity of cofilin-1. Rhodamine-labeled F-actin was polymerized and observed under a fluorescence microscope with 100x oil lens. The changes in both length and number of F-actin fibers were recorded over time with/without incubations of 1μM recombinant wild-type (wt) CFL1 and its S3A, DMA, or DMS mutant proteins. Images of one representative experiment are shown for each group. The length and number of F-actin at 5min of incubation were quantified. Data (mean ± SEM) were summarized in lower graph from three independent experiments, in which short (≤ 1μm) and long (> 1 μm) F-actin were averaged. Bars with different letters differ with each other significantly ($P < 0.05$). Scale bar = 5μm.

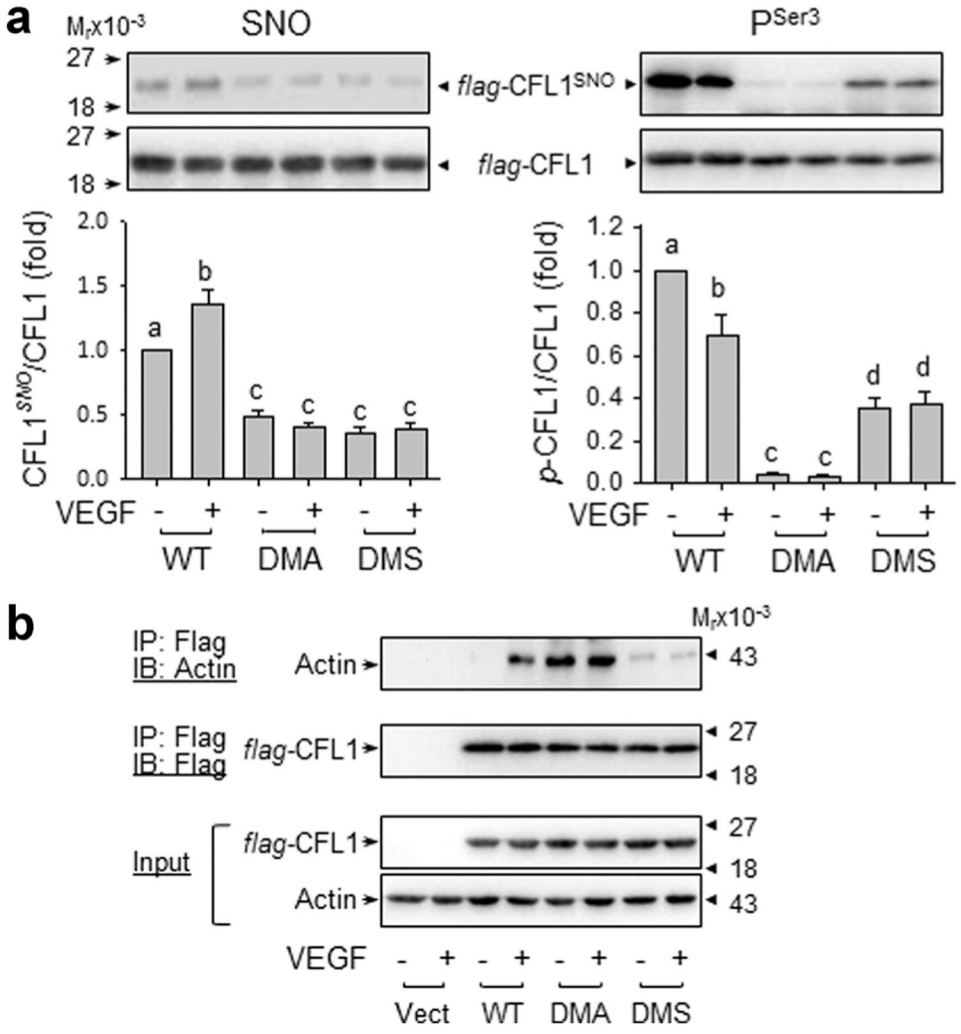

Fig. 4.

Effects of *SNO*-mimetic/deficiency on cofilin-1 phosphorylation. Flag-taggedwt-CFL1 and its DMA and DMS mutants were overexpressed in oFPAEC. Following treatment with 10 ng/ml VEGF, total cell lysates were harvested for determining changes in S-nitrosylation and phosphorylation of CFL1 (a) and CFL1-actin binding (b). Normalized data (mean ± SEM) from three independent experiments using oFPAEC from different pregnant ewes were summarized in graphs (a). Bars with different letters differ significantly ($P < 0.05$). Blots of a typical experiment (b) represent three similar independent experiments using cells from different pregnant ewes.

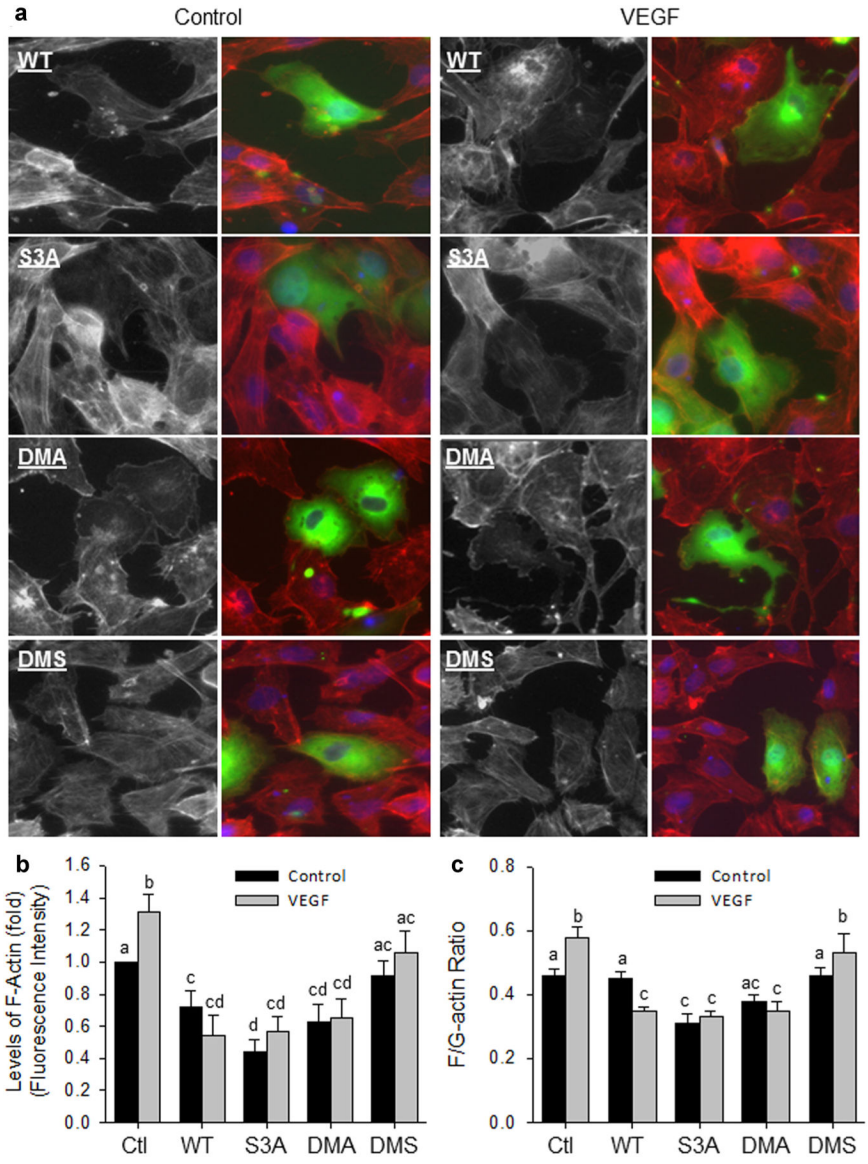

Fig. 5.

S-nitrosylation of cofilin-1 regulates F-actin formation in endothelial cells. Flag-tagged wt-CFL1 and its S3A, DMA, and DMS mutants were overexpressed in oFPAEC. After treated with/without 10 ng/ml VEGF for 24 h, the cells were fixed for labeling F-actin with TRITC-phalloidin and flag-CFL1 with FITC-conjugated anti-Flag antibody. Double fluorescence images (a) were captured for measuring the relative fluorescence intensities of F-actin by using SimplePCI software. Levels of F-actin (mean red fluorescence intensity) of 50 cells per group were obtained and summarized in graph (b). (c) The F/G-actin ratios in oFPAEC overexpressing wt-CFL1 and its mutants treated with/without 10 ng/ml VEGF for 30 min were determined. Graphs summarized data (mean ± SEM) from three independent experiments using oFPAEC from different pregnant ewes. Bars with different letters differ with each other significantly ($P < 0.05$). Scale bar = 20 μm.

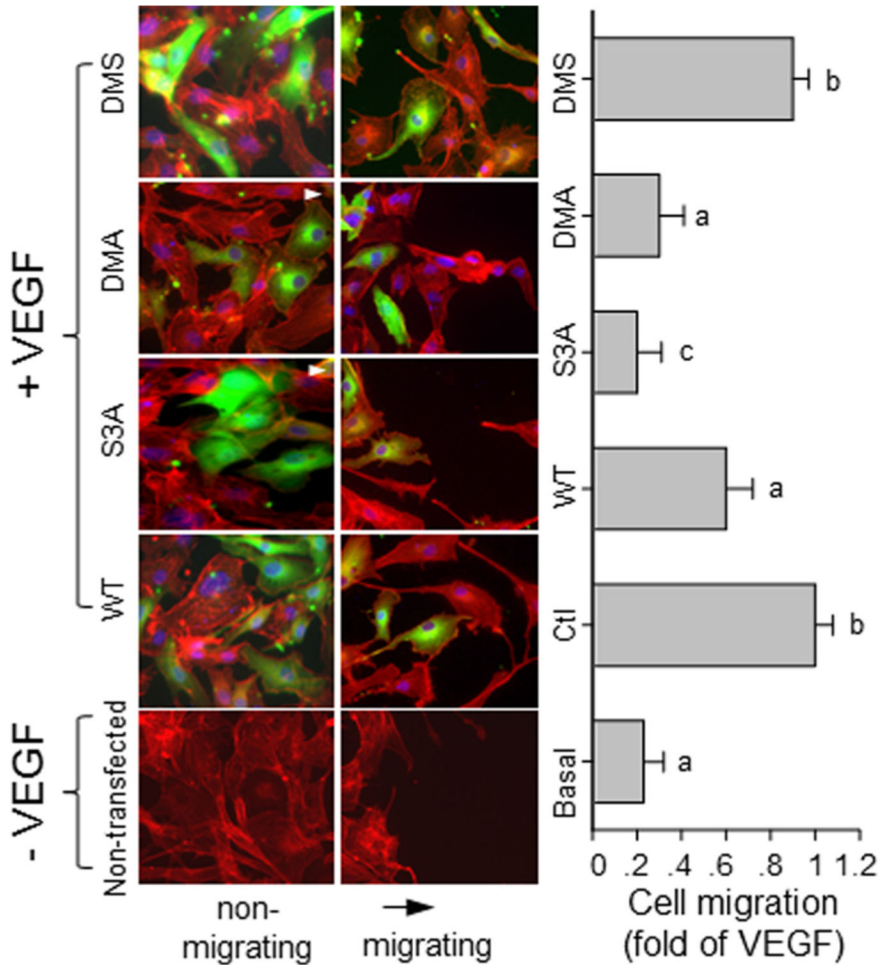

Fig. 6.

S-nitrosylation of cofilin-1 regulates endothelial cell migration. Flag-taggedwt-CFL1 and its S3A, DMA, and DMS mutants were overexpressed in oFPAEC. The cells were subjected to scratch wound cell migration assay with/without treatment with 10 ng/ml VEGF for 24 h. The cells were fixed for labeling F-actin with TRITC-phalloidin and flag-CFL1 with FITC-conjugated anti-Flag antibody. Fluorescence images were captured for demonstrating migrating cells at the leading edges of wounded areas and non-migrating confluent cells. Arrows indicates the direction of cell migration. The migration distances of transfected cells (red/green labeled) treated with VEGF in each group were measured and normalized as a ratio to that of the non-transfected (labeled in red) cells in the same group (control). Images of one typical experiment represent three similar experiments using cells from different pregnant ewes. Graph summarized data (mean ± SEM) from three independent experiments. Bars with different letters differ significantly ($P < 0.05$). Scale bar = 50 μm.

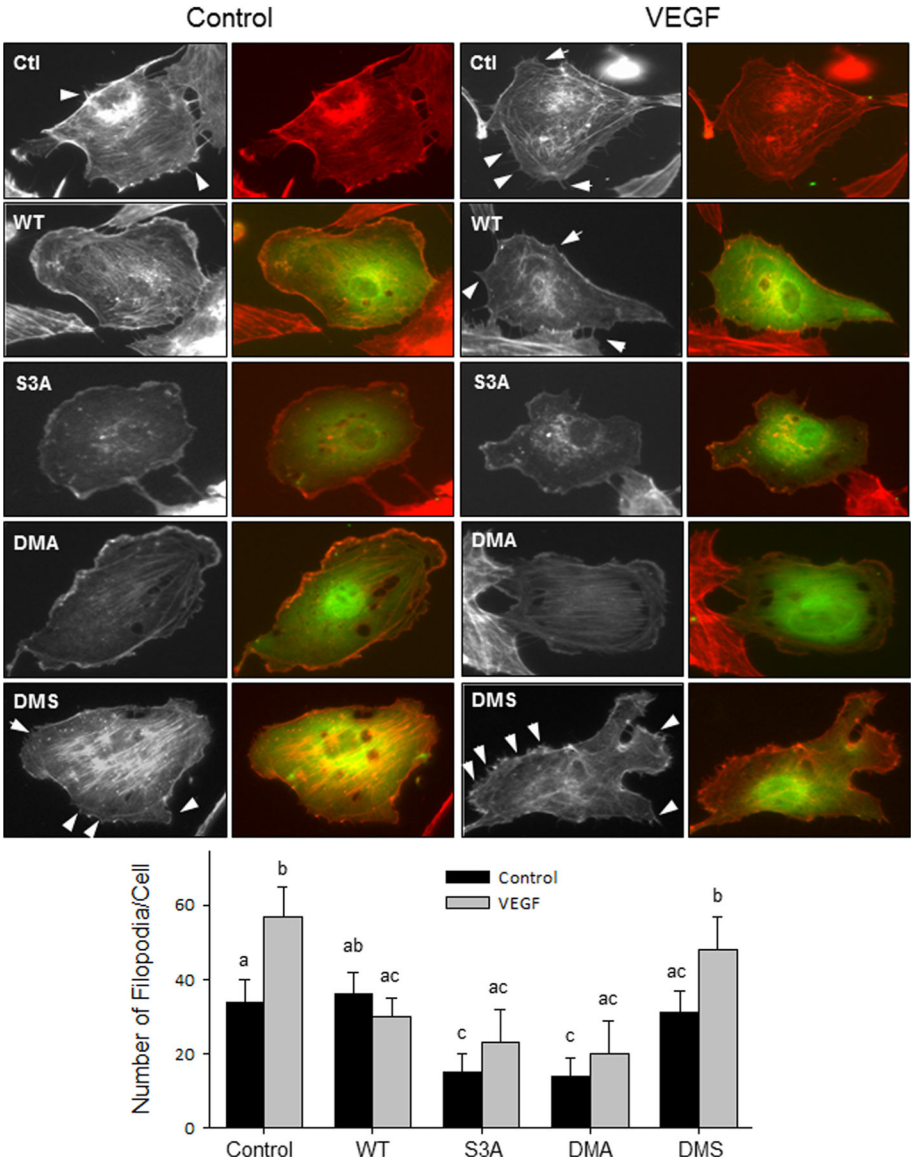

Fig. 7.

S-nitrosylation of cofilin-1 regulates filopodium formation in endothelial cells. Flag-tagged wt-CFL1 and its S3A, DMA, and DMS mutants were overexpressed in oFPAEC. Following treatment with 10 ng/ml VEGF for 24 h, the cells were fixed for labeling F-actin with TRITC-phalloidin and flag-CFL1 with FITC-conjugated anti-Flag antibody. Black white images show TRITC-labeled F-actin and color images show both F-actin and FITC-labeled Flag-CFL1. Arrows indicate typical filipodia in the cells. The average number of filopodium/cell of 30 cells in each group was quantified. Graph summarized data (mean ± SEM) from three independent experiments using cells from different pregnant ewes. Bars with different letters differ significantly ($P < 0.05$). Scale bar = 20 μm.

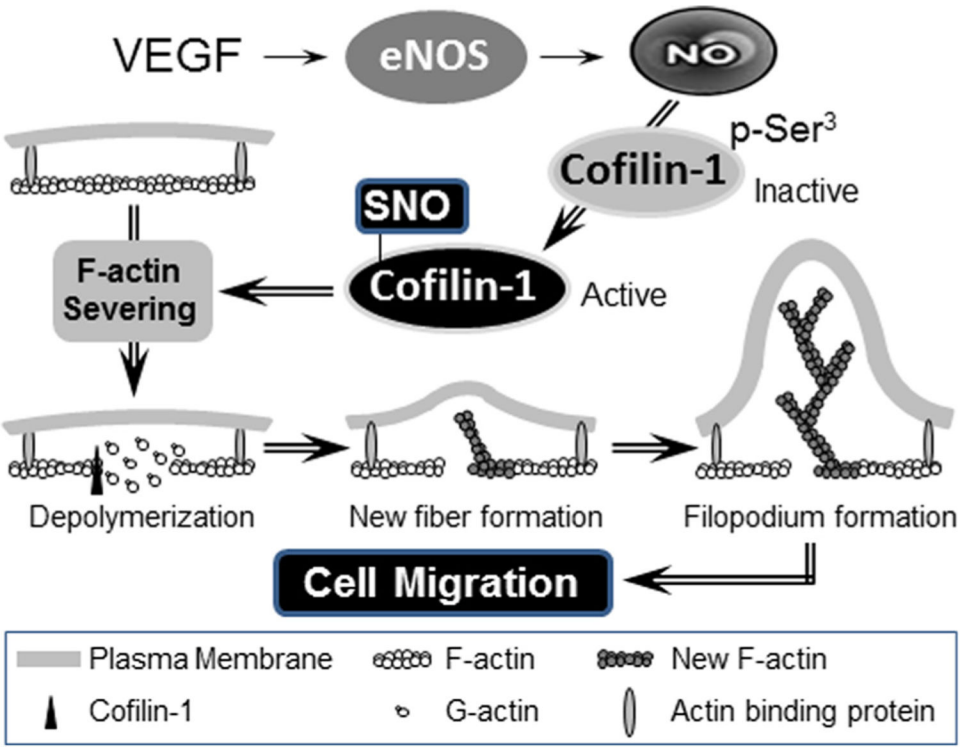

Fig. 8.

A novel pathway *post*-NO biosynthesis for mediating VEGF-induced endothelial cell migration via S-nitrosylation. VEGF stimulates dynamic S-nitrosylation of CFL1 via eNOS-derived NO, resulting in increased actin severing activity of CFL1 for regulating actin dynamics and cytoskeleton remodeling as well as migration in endothelial cells.